JOURNAL OF MATERIALS SCIENCE **38** (2003) 689–692

Amorphous boron nanoparticles and BN encapsulating boron nano-peanuts prepared by arc-decomposing diborane and nitriding

P. Z. SI, M. ZHANG, C. Y. YOU, D. Y. GENG, J. H. DU, X. G. ZHAO, X. L. MA, Z. D. ZHANG
Shenyang National Laboratory for Materials Science and International Centre for Materials Physics, Institute of Metal Research, Chinese Academy of Sciences, Shenyang 110016, People's Republic of China
E-mail: pzsi@imr.ac.cn

Amorphous boron nanoparticles were prepared by arc-decomposing diborane, which had ideal morphologies in comparison with that of those fabricated by furnace or laser heating diborane. Peanut-shaped boron nitride encapsulating boron nanocapsules were fabricated by nitridation of amorphous boron nanoparticles. Unique core/void/shell structure of the nanocapsules was observed by using a high-resolution transmission electron microscopy. The mechanism of growing the BN nanocapsules by a catalyst free process was distinctly different from the process of arc discharge or laser heating. The broadening of nonpolar intralayer Raman line of hexagonal BN at about 1370 cm^{-1} was observed, which was attributed to the small crystal size of BN.

1. Introduction

Boron chemistry includes many technical applications such as nuclear reactor control, pyrotechnic flares, rocket igniter, semiconductors, protective coatings and refractory materials. Elementary boron is commonly prepared by the reduction of boron compound with hydrogen or magnesium. High purity amorphous boron nanoparticles with broad size distribution (25–500 nm) in sufficient quantity for use were first synthesized by furnace heating diborane(∼700°C) [1]. Amorphous boron nanoparticles prepared by laser heating diborane (∼1400°C) show also non-ideal morphologies (i.e., chains and clusters) [2]. It was anticipated that the non-ideal morphologies would be improved by increasing the reaction-zone temperature [2], but no report of experiments on this topic yet. In this Letter, we fabricated successfully the amorphous boron nanoparticles with a narrow size distribution and ideal morphologies by arc decomposing diborane (>2500°C). On the other hand, boron nitride (BN) nano-materials have attracted great interests, due to their unusual properties in many respects such as high temperature structural stability, high resistance against acid corrosions, gas storage, etc. since the successful synthesis of BN nanotubes [3]. Besides interests on BN nanotubes [3–5], the formation of nanocapsules of *h*-BN encapsulating metal/oxides, including cobalt oxides [6], gold, iron oxide and germanium [7], Zr compounds [8] and silver/oxides [9] have been reported. This work enlarged the family of BN nanocapsules with different cores and shapes. Boron nitride encapsulating boron nanocapsules were fabricated by nitridation of the amorphous boron nanoparticles.

Most of techniques for synthesizing BN nanomaterials involve a catalyzed high temperature and/or high gas pressure process, among which arc discharge and arc-melting process [3, 6] are commonly used. Chen *et al*. synthesized BN nanotubes by the combination of reactive ball milling and post annealing of disordered BN [10]. Usually, BN nanotubes grow from nanoparticles of metal [3] or metal oxide [5], pure BN crystal [11] or BN crucible [12], which serve as catalysts or seeds. The operational easiness and the less contamination from free catalysts of the present method are benefit to potential large-scale applications.

2. Experimental procedure

A traditional nanoparticles generator with a cylindrical water-cooled chamber (Φ280 mm × 400 mm) was employed for the fabrication of amorphous boron nanoparticles. A flexible tungsten needle of 2 mm in diameter served as the cathode. The anode was a bulk iron lying in the water-cooled copper stage. The chamber was evacuated to 0.0013 Pa before the introduction of a mixture of argon (purity 99.9%, 24000 Pa) and diborane (purity 99.7%, 5700 Pa). An arc with a typical current of 20 ampere, maintaining for 10 seconds, was struck between the tungsten electrode and the anode. The nanoparticles collected from the wall in air were used for TEM observations and subsequent synthesis of BN nanocapsules in a conventional furnace using silicon carbide rods as heaters. The fine particles were first laid down on an aluminium oxide boat, and then put in the central region of a silica tube (Φ0.05 × 1 m)

surrounded by heater rods. After that, pure nitrogen ($\sim$0.0001 m^3/min) was introduced into the silica tube to drive out oxygen inside the tube. One hour later, the tube isolated from air by flowing N_2 and by water sealing was heated at a rate of 10°C/min to 1100°C and maintained at this temperature for 5 hours. Finally, the sample was cooled down to room temperature under pure N_2.

X-ray diffraction (XRD) patterns were recorded in a D/max-γA diffractometer with Cu K_α radiation. The structures were observed by using a JEM2010 high-resolution transmission electron microscopy (HRTEM) operating at 200 kV with the magnifications of 40 K, 80 K and 500 K. The samples for TEM observations were prepared by first dispersing the powders in alcohol with ultrasonic field for 20 minutes, then picking one drop of the suspension on a carbon-coated TEM mesh grid. A vibrating sample magnetometer (VSM) was used to detect the possible magnetic impurities in the particles. Raman scattering spectra were recorded from 800 to 2000 cm^{-1} frequency shift in the Stokes region, using a 632.817 nm laser for excitation.

3. Results and discussion

3.1. Characterization of amorphous boron nanoparticles

The diameter of the spherical particles synthesized by cracking diborane is 75 nm in average, with a narrow size distribution (55–95 nm) as shown in Fig. 1. The narrow size distribution (compared with [1]) and ideal shape (compared with [1, 2]) should be attributed to the high temperature of the arc, as Casey and Haggerty anticipated [2]. Boric acid crystalline was detected by XRD, which was attributed to the reaction between the remains of B_2H_6 in the chamber and the moisture in the air when collecting the particles. No iron from anode was detected in the particles by both XRD and VSM. Similar experiments using bulk iron as the argon arc target produced merely 260 mg Fe nanoparticles in 5 hours. Thus the iron contamination was estimated to be as low as 0.03 wt% comparing with the 450 mg products prepared by arc-cracking diborane in 10 seconds.

3.2. Characterization of products prepared by nitriding amorphous boron nanoparticles

Fig. 2 shows XRD patterns of boron nanoparticles annealed under flowing nitrogen at 1100°C. The broadening nature of the XRD peaks indicates that the grain size is on nanometer scale and/or the amorphous phases exist. The hexagonal boron nitride is the main phase of the sample, coexisting with boric acid and α-boron as minority phases. Unknown peaks are thought to be the result of contaminations from crucible and furnace at high temperatures. The existence of α-boron is due to the decrease of the crystallization temperature of the amorphous boron nanoparticles, compared to that of bulk amorphous boron [13]. The formation mechanism of boric acid in the annealed samples was elucidated as follows. First, the oxygen introduced by boric acid in the as-synthesized samples could not be separated out, even at the temperature as high as 1100°C. Second, the oxygen impurities in the nitrogen could react easily with boron nanoparticles according to the reaction of

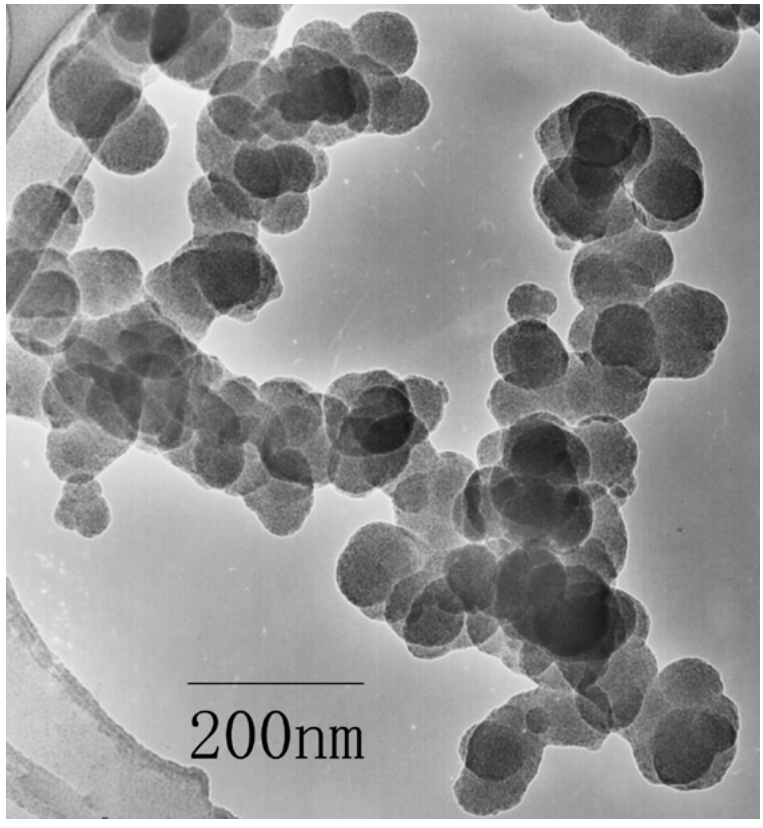

Figure 1 Transmission electron micrograph of amorphous boron nanoparticles synthesized by arc decomposing diborane, showing an average diameter of 75 nm and a narrow size distribution.

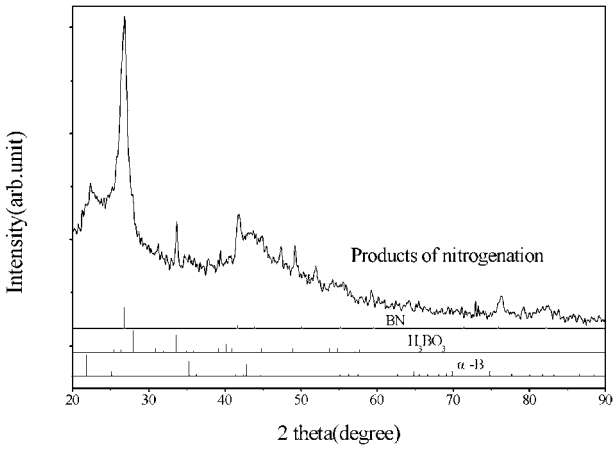

Figure 2 XRD patterns of products prepared by nitridation of boron nanoparticles at 1100°C for 5 hours, which show the main phase of BN with trace amount of α-B and boric acid.

$4B + 3O_2 \rightarrow 2B_2O_3$ at high temperatures [14]. B_2O_3 would react spontaneously with moisture in the air to form boric acid phase at room temperature, because the free Gibbs energy of the reaction of $B_2O_3 + H_2O \rightarrow H_3BO_3$ is negative.

A TEM image in Fig. 3a exhibits a general view of *h*-BN nanocapsules. The dominant products are nanocapsules with spherical and polyhedral peanut shapes, which consist in general of a crystal/amorphous boron core—appearing with a darker contrast in the image—encapsulated by a BN shell. The voids appear in between the core and shell as bright contrast in the image, which are different from other nanocapsules in shapes [6–9]. The diameter of the nanocapsules ranges from 20 to 130 nm. The thickness of the shell is approximately 10 nm, while that of the voids sandwiched in between the shell and core is 16 nm or less. Nanocapsules with elongated or peanut shapes are attributed to the surface contact of different nanoparticles during nitriding.

The formation of multilayered BN shell by nitriding boron nanoparticles has been confirmed by a HRTEM image in Fig. 3b. Lattice fringes, originating from *c* planes of *h*-BN parallel to the incident electron beam, are observed around the boron nanoparticles. The spacing of 0.332 nm for equally separated BN layers is consistent with the inter-planar distance of 0.333 nm in bulk *h*-BN. The cores being encapsulated by BN layers are crystal/amorphous boron and voids. The general intersection views of the nanocapsules as seen by the TEM are little different according to the size of nanoparticles. The shell/core phase separations, i.e. the voids, are obviously seen for the capsules with the size of approximately 100 nm as shown in Fig. 3a. However, as shown in Fig. 3b, it is hard to observe phase separations for nanocapsules with diameters of about 20–30 nm.

The nonpolar intralayer Raman line of hexagonal BN at about 1370 cm^{-1} was observed, as shown in Fig. 4. The broadening of this line was attributed to the small crystal size of BN as described by Nemanich [15]. The upshift of the Raman line with decreasing crystal sizes described in [15] is not observed here.

The clear phase separation, i.e. the appearance of the void, between the BN shell and the amorphous/crystal

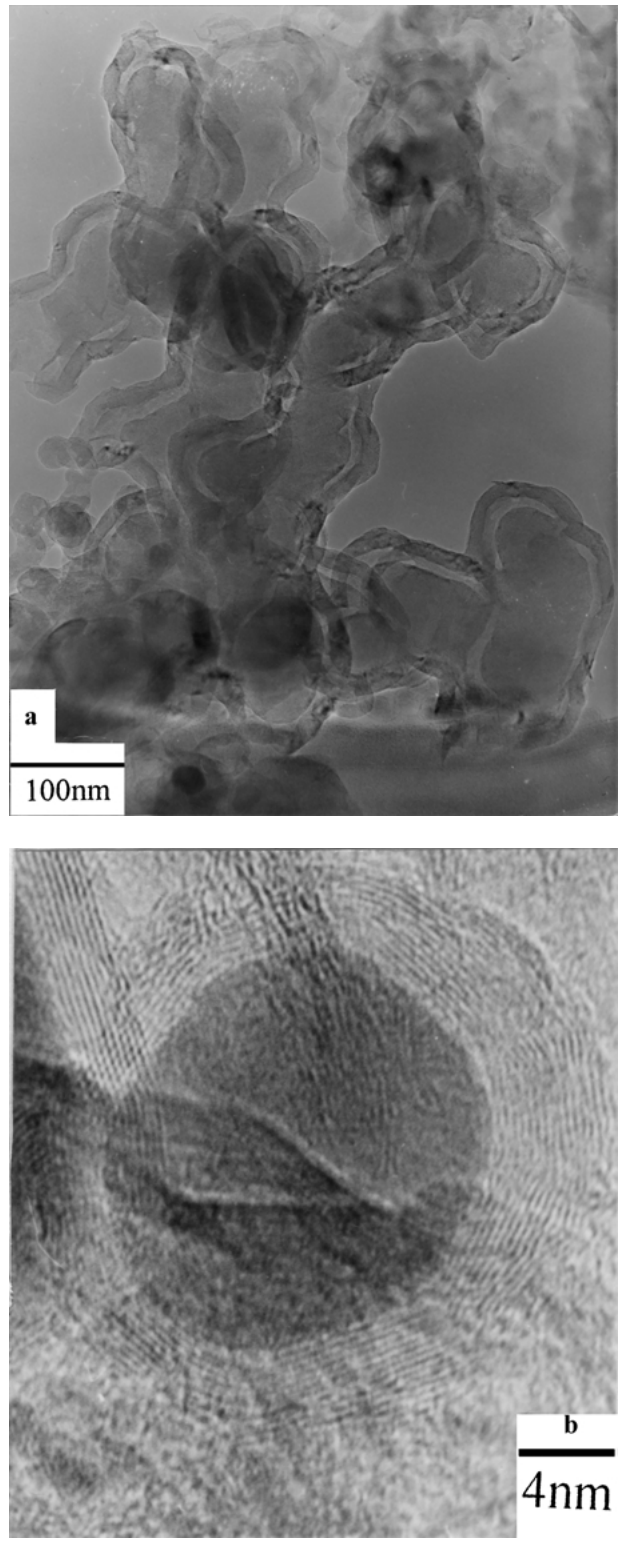

Figure 3 Morphology of the BN nanocapsules (a), showing spherical or elongated peanut shape BN encapsulating boron with void sandwiched in between nanocapsules, and HRTEM image of the small BN nanocapsules (b), showing 6–20 BN layers around the particles. The layers are equally separated with a spacing of 0.332 nm.

boron core raises the question of the growth mechanism itself. Here we present a two-step model to illustrate the formation process of the nanocapsules. Boron atoms at the surface of a nanoparticle first react with the nitrogen gas to form a locally BN layer, and then the BN layer grows along the surface of the boron nanoparticles until the whole particle is encapsulated inside. The reason for BN growing along the shell instead of the boron

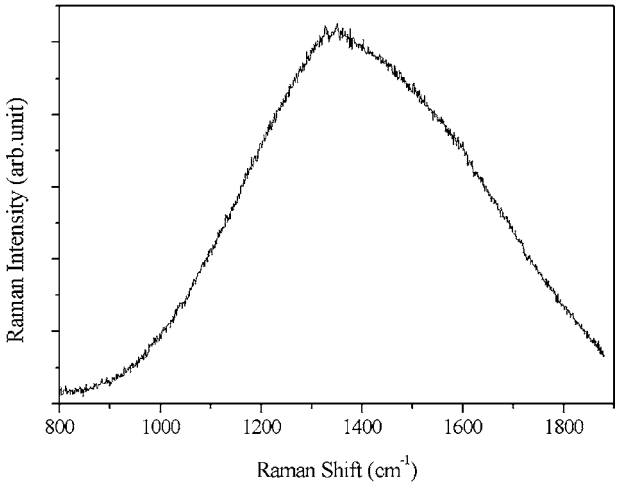

Figure 4 The Raman spectrum of BN encapsulating B nanocapsules.

core is that BN plays an important role as catalysts [12], which makes crystal growth easier on BN surface than on boron surface. In the next step, the boron atom evaporation and diffusion results in that boron react with nitrogen gas at the surface of the BN shell. As a result, a void space forms between the shell and the core.

Different thermal expansion coefficients of BN and B may also involve in the void formation. R. S. Pease gave temperature dependence of hexagonal BN lattice parameters expressed in Angstrom units

$$c = 6.6516 + 2.74 \times 10^{-4} t \quad \text{and}$$
$$a = 2.50424\text{–}7.42 \times 10^{-6} t + 4.79 \times 10^{-9} t^2,$$

where t is the temperature in degrees centigrade [16]. Therefore the c dimension contracts 4.26% while the a dimension expands 0.089% from 1100°C to 20°C. Boron has a coefficient of thermal expansion of about 8.29×10^{-6} deg.$^{-1}$ [17], indicating a linear contraction of 0.9% when temperature drops from 1100°C to 20°C. As a result, the maximum void formed this way should be no more than 0.989% in dimensions. Of course, the phase transformation from amorphous boron to an ordered α-boron lattice will lead to shrinkage in volume and thus an enlarging in void. We believe that a long enough annealing time will result in the completely disappearance of boron and thus the formation of hollow BN nano-peanuts. The void formed this way could give a good place for gas storage [6]. Since the present BN nanocapsules consists of only light elements, it is believed that they can store much gas per weight. Moreover, the shapes and the sizes of nanocapsules largely depend on the shape and particle size of the starting materials, which give a promising prospect for manufacturing different types of BN nano-parts by controlling the shapes of the starting materials.

4. Conclusions

The amorphous boron nanoparticles with a narrow size distribution and ideal spherical morphologies have been fabricated by arc decomposing diborane. The high temperature of the arc and the ideal spherical morphologies has to some extent supported the anticipation given by Casey and Haggerty [2]. The new shell/void/core structured nano-materials—BN encapsulating void and boron—have been fabricated successfully. Simple nitriding method employed gives potential large-scale industrial applications in field like nano-manufacturing. The metal/oxide catalyst free process for formation of BN encapsulating B nano-materials can to some extent reduce the contamination of the BN products.

Acknowledgement

We gratefully acknowledge the financial support from the National Natural Science Foundation of China (Grants No. 59725103 and No. 50171070) and the Science and Technology Commission of Shenyang.

References

1. H. L. JOHNSTON, H. N. HERSH and E. C. KERR, *J. Amer. Chem. Soc.* **73** (1951) 1112.
2. J. D. CASEY and J. S. HAGGERTY, *J. Mater. Sci.* **22** (1987) 737.
3. N. G. CHOPRA, R. J. LUYKEN, K. CHERREY, V. H. CRESPI, M. L. COHEN, S. G. LOUIE and A. ZETTL, *Science* **269** (1995) 966.
4. Y. SAITO, M. MAIDA and T. MATSUMOTO, *Jpn. J. Appl. Phys.* **38** (1999) 159.
5. D. GOLBERG and Y. BANDO, *Appl. Phys. Lett.* **79** (2001) 415.
6. M. KUNO, T. OKU and K. SUGANUMA, *Scripta Mater.* **44** (2001) 1583.
7. T. HIRANO, T. OKU, M. KAWAGUCHI and K. SUGANUMA, *Molecular Crystals Liquid Crystals.* **340** (2000) 787.
8. Y. SAITO, M. MAIDA and T. MATSUMOTO, *Jap. J. Appl. Phys.* P1. **38** (1999) 159.
9. T. OKU, T. KUSUNOSE, T. HIRATA, R. HATAKEYAMA, N. SATO, K. NIIHARA and K. SUGANUMA, *Diamond Related Mater.* **9** (2000) 911.
10. Y. CHEN, J. F. GERALD, J. S. WILLIAMS and S. BULCOCK, *Chem. Phys. Lett.* **299** (1999) 260.
11. D. GOLBERG, Y. BANDO, M. EREMETS, K. TAKEMURA, K. KURASHIMA and H. YUSA, *Appl. Phys. Lett.* **69** (1996) 2045.
12. M. TERAUCHI, M. TANAKA, H. MATSUDA, M. TAKEDA and K. KIMURA, *J. Electron Microsc.* **1** (1997) 75.
13. S. O. SHALAMBERIDZE, G. I. KALANDADZE, D. E. KHULELIDZE and B. D. TSURTSUMIA, *J. Solid State Chem.* **154** (2000) 199.
14. D. H. RIU, R. CHOI, H. E. KIM and E. S. KANG, *J. Mater. Sci.* **30** (1995) 3897.
15. R. J. NEMANICH, S. A. SOLIN and R. M. MARTIN, *Phys. Rev.* B. **23** (1981) 6348.
16. R. S. PEASE, *Acta Cryst.* **5** (1952) 356.
17. P. T. B. SHAFFER, in "Plenum Press Handbooks of High-temperature Materials" (Plenum Press, New York, 1964) p. 191.

Received 3 June
and accepted 1 October 2002